OPTICAL REVIEW Vol. 17, No. 3 (2010) 275–281

Wavelength-Tunable Multicolored Femtosecond Laser Pulse Generation in a Fused Silica Glass Plate

Takayoshi KOBAYASHI[1,2,3,4] and Jun LIU[1,2]

[1]*Department of Applied Physics and Chemistry and Institute for Laser Science, University of Electro-Communications, 1-5-1 Chofugaoka, Chofu, Tokyo 182-8585, Japan*
[2]*International Cooperative Research Project (ICORP), Japan Science and Technology Agency, 4-1-8 Honcho, Kawaguchi, Saitama 332-0012, Japan*
[3]*Department of Electrophysics, National Chiao Tung University, 1001 Ta Hsueh Rd., Hsinchu 300, Taiwan*
[4]*Institute of Laser Engineering, Osaka University, 2-6 Yamadaoka, Suita, Osaka 565-0871, Japan*

(Received September 19, 2009; Accepted January 17, 2010)

We obtained an array of multicolored femtosecond laser pulses with as many as 17 different colors that are spatially isolated. The mechanism of generation was proved to be cascaded four-wave mixing and with the following procedure. The output beam from a femtosecond laser was split into two. One of the two beams was pulse-compressed with a hollow core fiber and the intensity of the other was reduced. The two beams were synchronized and combined with a small crossing angle in a plate of fused silica glass plate. The wavelengths of the sidebands are continuously tunable from near-ultraviolet to near-infrared. The pulse duration, spatial mode, spectrum, and energy stability of the sidebands were studied. As many as fifteen spectral up-shifted pulses and two spectral downshifted pulses were obtained with spectral bandwidths broader than 1.8 octaves. Properties such as pulse energy as high as 1 μJ, 45 fs pulse duration, smaller than 1.1 times of the diffraction limit Gaussian spatial profile, and better than 2% RMS power stability of the generated sidebands make it can be used in various experiments. The characterization showed that the sidebands have sufficiently good qualities to enable application to for various multicolor femtosecond laser experiments, for example, a multicolor pump-probe experiment.

Keywords: four-wave mixing, multicolor, femtosecond

1. Introduction

Optical parametric amplification based on three-wave mixing in second-order nonlinear crystals had been studied extensively in the past decade. The generation method of tunable femtosecond laser pulses from near-ultraviolet to near-infrared (NUV to NIR) has been well established by using this type of method and is widely used in pump-probe experiments.[1)] Sub-two-cycle ultrashort pulses were generated in visible[2)] and NIR[3)] regions through non-collinear optical parametric amplification (NOPA) in a β-BaB_2O_4 (BBO) crystal by using noncollinear configuration of phase matching.

Recently, an ultrabroadband spectrum and ultrashort pulses were generated by adopting four-wave mixing (FWM) driven by third-order susceptibility, in various optically transparent media. Tunable visible ultrashort pulses were generated by FWM through filamentation in a gas cell.[4)] Femtosecond ultrashort pulses, even in both deep UV (DUV) and in NIR, were generated by FWM through filamentation in gases.[5,6)] For bulk solid-state media, phase matching can be obtained only if the pump beams have a finite crossing angle owing to high material dispersion. Sideband signals due to cascaded FWM were generated in a BK7 glass plate[7)] and a sapphire plate[8)] with two crossing femtosecond laser beams. Different-frequency resonant FWM, named coherent anti-stokes Raman scattering (CARS), took place and broadband sidebands with high-efficiency were generated in some nonlinear crystals.[9–14)] Upon using ps pump pulses, high-efficiency, high-energy noncollinear four-wave optical parametric amplification in a transparent bulk Kerr medium was also observed.[15,16)] In comparison with the three-wave mixing process, FWM is more flexible and more widely applicable to nearly every transparent medium in a broad spectral range. This is because the FWM phase-matching requirement is more flexible because of the great number of frequencies involved and also, symmetry is not required in the third-order optical nonlinear process.

In some types of experiment, for example, femtosecond CARS spectroscopy,[17)] two-dimensional spectroscopy[18)] and high-intensity laser experiments,[19)] two or more femtosecond pulses at different wavelengths are needed. Usually, separate NOPA systems are set up to obtain the required femtosecond pulses at different wavelengths and then these NOPA pulses are synchronized.[20)]

In this letter, we report on the experimental generation of wavelength-tunable multicolored femtosecond laser pulses in fused silica glass. Femtosecond laser pulses at different wavelengths were generated at the same time by the cascaded FWM process. Then, the setup is simplified compare to that of the multicolor femtosecond laser obtained by NOPA systems. The wavelength of the generated pulses can be tuned by changing the crossing angle of the two input beams on the glass. The generated femtosecond sidebands have a Gaussian spatial profile, as small as 1.1 times diffraction limit (DL), and 2% RMS energy stability, which can be used in different kinds of multicolor pump-probe experiments.

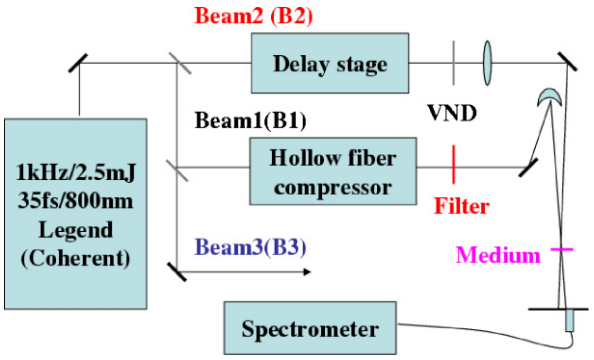

Fig. 1. (Color online) Schematic of experimental setup. VND: variable neutral-density filter. Filter: bandpass filter at 700 nm center wavelength with 40 nm bandwidth or short pass filter cutting at 800 nm. Medium: 1-mm-thick fused silica glass plate.

2. Experimental Setup

The schematic of the experimental setup is shown in Fig. 1. A 1 kHz Ti:sapphire regenerative amplifier fs laser system (Coherent Micra+Legend-USP) with 35 fs pulse duration, and 2.5 W average output power was used as the pump source. The laser beam after the regenerative amplifier system was split into several beams using beam splitters. One beam (beam1) was spectrum broadened in a krypton-gas-filled hollow fiber with the inner diameter of 250 μm and the length of 60 cm. The broadband spectrum after the hollow fiber was dispersion compensated with a chirped mirror pair and a pair of glass wedges. The shortest pulse duration after the hollow-fiber compressor was about 10 fs. After passing through a short-wavelength edge pass filter cut at 820 nm and a variable neutral-density (VND) filter, beam1 was focused onto 1-mm-thick fused silica glass with a concave mirror. Another beam (beam2) passed through a delay stage with less than 3 fs resolution. Beam2 was first attenuated by a VND filter and then focused onto the fused silica glass with a lens. The third beam (beam3) was used to generate cross-correlation signals with the two input beams and the generated sidebands in a 10-μm-thick BBO crystal that was used to measure their pulse durations.

3. Experimental Results and Discussion

3.1 Four-wave mixing experiment with no specific control of spatial, temporal, or spectral overlaps

At first, the four-wave mixing experiment without any specific control of overlaps in space, time and the spectra between the two beams was carried out. In the experiment, the width of the cross-correlation between beam2 and beam3 was measured to be 82 ± 5 fs, as shown in Fig. 2(a). The cross-correlation width between beam1 and beam3 was increased to 165 ± 10 fs owing to group velocity delay (GVD) in the VND and lens, as shown by the triangles in Fig. 2(b). The diameter of the two input beams on the surface of the fused silica glass was measured to be 180 μm with a charge coupled device (CCD) camera (Ophir Optronics BeamStar FX 33), as shown in the inset of Fig. 3. Then, the two beams were tuned so as to overlap by monitoring with the

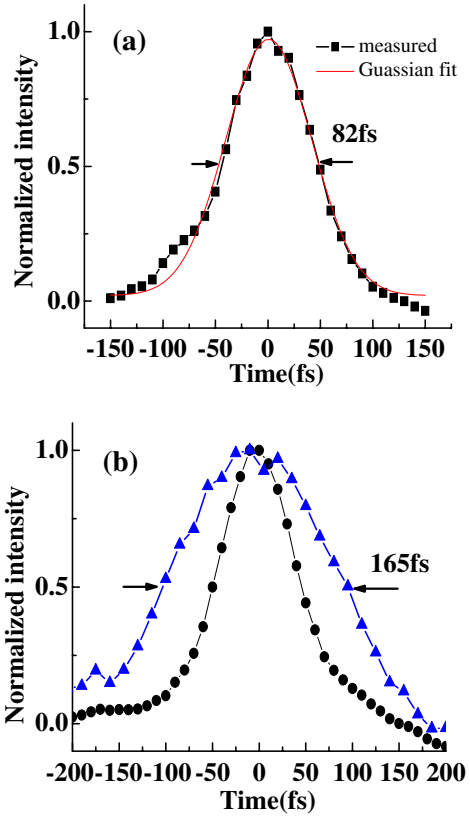

Fig. 2. (Color online) Cross-correlation width between one of the two input beams and beam3. (a) Beam2 and beam3: 82 ± 5 fs. (b) Beam1 and beam3, triangles: 165 ± 10 fs, filled circles: 84 ± 5 fs.

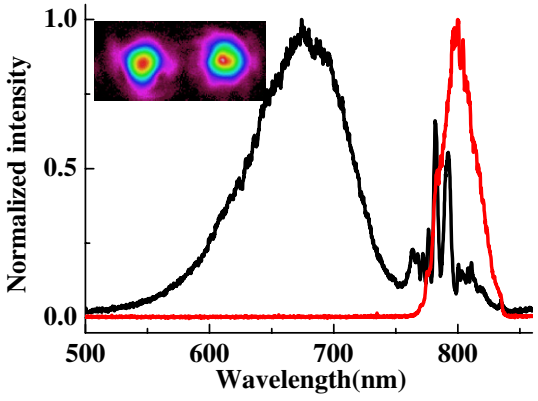

Fig. 3. (Color online) Spectra of two input beams before incidence to the fused silica glass. Black line: beam1, red line: beam2. The inset depicts the spatial mode patterns of the two input beams on the surface of the glass. The left and right pattern are for beam1 and beam2, respectively.

CCD. Figure 3 shows the spectra of beam2 and beam1 in front of the fused silica glass. By using the hollow fiber compression system, it is easy to generate a laser pulse with a broadband spectrum on the both sides of 800 nm and with high energy. Such a broadband spectrum and high energy of the pulse make it possible to generate wavelength-tunable FWM sidebands with relatively high pulse energy.

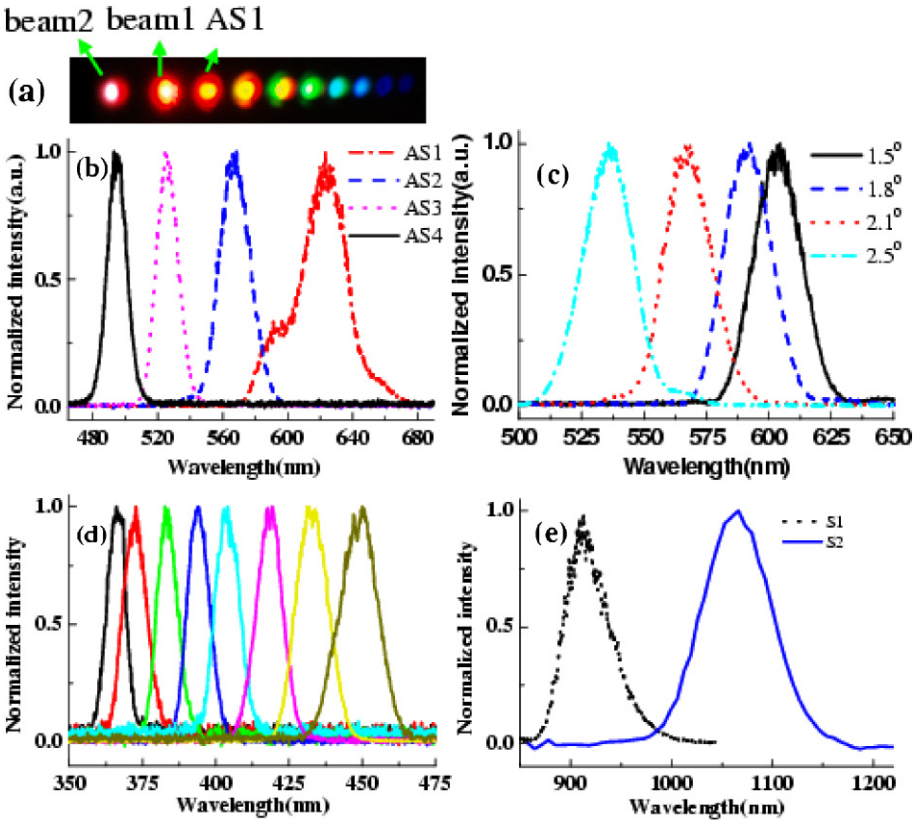

Fig. 4. (Color online) (a) Photograph of sidebands on a sheet of white paper 1 m after the glass plate. (b) Spectra of sidebands from AS1 to AS4 when crossing angle was 2.1°. (c) Spectra of AS2 at four different crossing angles of 1.5, 1.8, 2.1, and 2.5°. (d) Spectra of high-order anti-Stokes signals from AS15 to AS8 and (e) two Stokes signals when the crossing angle was about 1.5°.

As beam1 and beam2 were synchronously focused on the fused silica glass both in time and space, separated cascaded FWM signals at different wavelengths were generated beside the input beams. Figure 4(a) shows a photograph of the FWM sideband signals on a sheet of white paper placed about 1 m from the glass plate. The first two beams on the left side were the two input beams, beam2 and beam1 from left to right, respectively. The input powers of beam1 and beam2 were 11 and 19 mW, respectively. The polarization of the two input beams and the sidebands were all checked to be parallel. Figure 4(b) shows the spectra of the wavelengths from the first-order (AS1) to the fourth-order anti-Stokes (AS4) FWM signals when the crossing angle between the two input beams was 2.1°. As we can see, the spectra extend from 475 to 675 nm. Each spectrum has a Gaussian profile and bandwidth of about 600 cm^{-1}, which supports the transform-limit pulse duration of 25 fs. Moreover, the wavelength of the sidebands can be tuned by changing the crossing angle between the two input beams. It can be seen from Fig. 4(c) that the spectra of AS2 can be tuned from 500 to 625 nm by changing the crossing angles between the two input beams from 1.5 to 2.5°. In Fig. 4(b), it was obvious that this tuning range fully covers the wavelengths of AS1 and AS3. In such a way, the spectra of the sidebands are able to be continuously tuned in a broadband range by changing the crossing angle between the two input beams. Some calculations based on this kind of FWM process have already been given.[7,15)]

In the experiment under certain conditions, as many as fifteen anti-Stokes signals and two Stokes signals with a spectrum extended from 360 nm to 1.2 μm for more than 1.8 octaves were obtained. For clarity, only the spectra of the high-order anti-Stokes and two Stokes signals (S1 and S2) are shown in Figs. 4(d) and 4(e). This means the sidebands can be tuned from the UV to NIR region in a broadband wavelength. Even though the pulse energy of the high-order anti-Stokes signal is low, the broadband spectrum is still of great interest. A nearly monocyclic pulse chain can be obtained from these broadband-cascaded FWM signals on the basis of the Fourier synthesis principle.[21)]

The pulse durations of AS1 and AS2 were measured by cross-correlation with beam3 from the Ti:sapphire laser system. When the cross-correlation width between beam1 and beam3 was 165 ± 10 fs [Fig. 2(b)], the cross-correlation width between AS1 and AS2 and beam3 were both 80 ± 5 fs, which is almost the same as the cross-correlation width of beam2, as shown in Fig. 5(a). We reduced the insertion length of the glass wedge in the hollow fiber compressor to compensate some dispersion generated by the filters in the beam path in order to reduce the pulse duration of beam1. We found that the pulse duration of AS1 was even shorter than that the two incident pulses, when the cross-

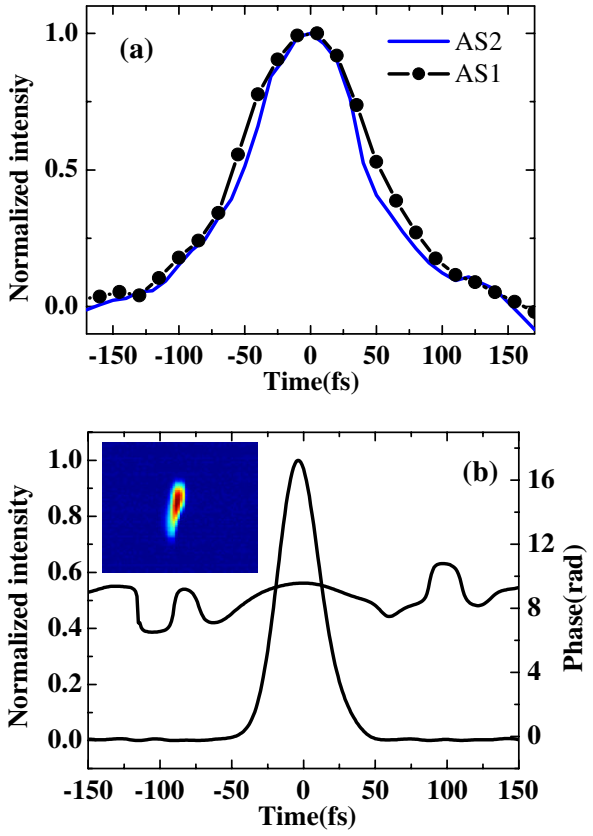

Fig. 5. (Color online) (a) Cross-correlation width of AS1 and AS2 when the cross-correlation width of beam1 was about 165 fs. (b) XFROG-retrieved trace of pulse duration and phase of AS1 when cross-correlation width of beam1 was about 84 fs. The pulse duration was about 35 fs. The inset shows the measured XFROG trace.

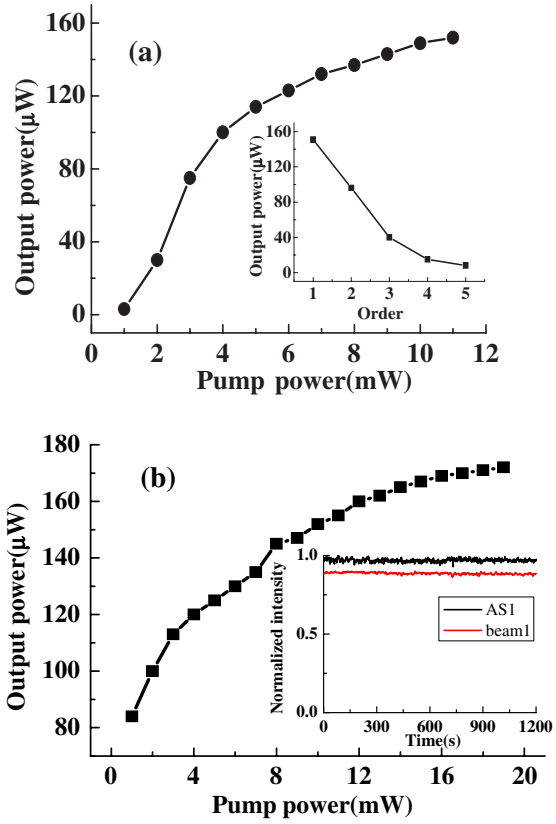

Fig. 6. (Color online) Dependence of the output power of AS1 on the power of one of the two input beams. (a) Dependence of beam1 power with the fixed power of 19 mW for beam2; (b) dependence of beam2 power with the fixed power of 11 mW for beam1. The inset of Fig. 5(a) depicts the output power of AS1 to AS5 when the input powers of beam1 and beam2 were 11 and 19 mW, respectively, and the crossing angle was 1.8°. The inset of Fig. 5(b) shows the power stability of AS1 and beam1 for half an hour.

correlation width of beam1 and beam3 was about 84 fs. Figure 5(b) shows the retrieved cross-correlation frequency-resolved optical gating (XFROG) pulse trace and phase of AS1 with a retrieved error of 0.018. The retrieved pulse duration was 35 ± 3 fs. The retrieved phase shows that there is still some chirp in the pulse owing to the positive chirped input pulses and the dispersion of the glass. It is expected that sidebands with much shorter pulse duration can be generated by using much shorter input laser pulses.

The output power of the sidebands was monitored with a silicon sensor power meter. The output power decreased from 153 to 8 μW as the order of the sidebands increased from AS1 to AS5, as shown in the inset of Fig. 6(a). The dependence of the AS1 output power on the power of the two input beams was also measured in the experiment. Figure 6(a) shows the dependence of the AS1 output power on the power of beam1 used as the pump beam in this cascade FWM process, while the power of beam2 was maintained at 19 mW and the crossing angle was 1.8°. The output power of AS1 was sensitive to the pump power of beam2. The output power of AS1 was found to be saturate as the pump power increased to about 11 mW. This saturation phenomenon can also be seen in Fig. 6(b). In that case, the power of beam1 was maintained to be 11 mW and the crossing angle was set at 1.5°. The AS1 output power was not so sensitive to the input power of beam2. The stabilities of the output powers of AS1 and beam1 were 3.1% RMS and 1.4% RMS, respectively, which were monitored simultaneously for half an hour during the experiment, as shown in the inset of Fig. 6(b).

Using a CCD camera, we measured the spatial profile of the generated sidebands. They all have a Gaussian spatial profile. AS1 is collimated and then focused by a lens with a focal length of 700 mm. From the formula $DL = 1.22\lambda f/D$ and the measured beam diameter at focal point, we found the beam quality was better than $1.1DL$. Figure 7 shows the two-dimensional and one-dimensional spatial profiles of the AS1 signals. The red dashed line depicts the Gaussian fitted line.

As mentioned above, we experimentally generated spectrally and spatially well-separated multicolored femtosecond laser pulses by using a cascade FWM process in a fused silica glass. The wavelength can be continuously tuned by changing the crossing angle between two input beams. From the results of the experiment, the properties of the generated pulses were reached to be good enough for different kinds of

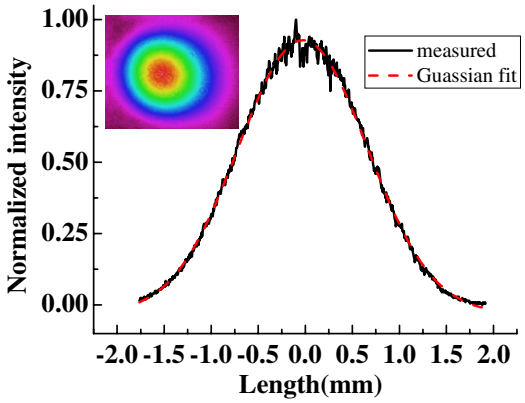

Fig. 7. (Color online) Spatial profile of AS1 beam (black solid line) and Gaussian fitted curve to the AS1 beam (red dash line). The inset shows the 2D spatial mode pattern of AS1 signal.

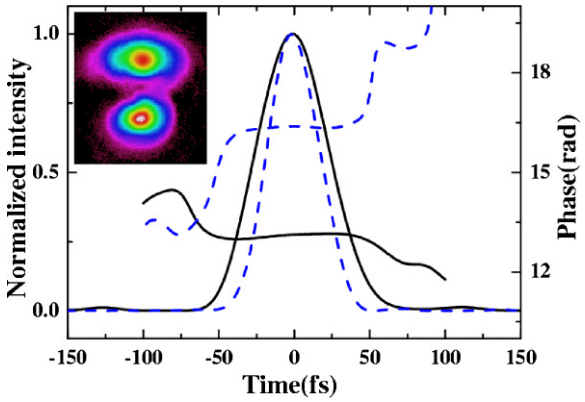

Fig. 8. (Color online) Input pulse duration and phase of beam1 (dashed lines) and beam2 (solid lines). The inset shows the two-dimensional beam profiles of beam1 (below) and beam2 (upper) on the surface of the fused silica glass.

experiments. The output power of the sidebands can be increased easily by increasing the input power. Moreover, it can also be amplified by using another four-wave optical parametric amplification system.[15] This method can be extended to be applied to different species of condensed isotropic media and to UV wavelength, which is difficult to be obtained using a nonlinear crystal because of the required condition of rigorous phase matching.

3.2 *Generation of μJ-level multicolored femtosecond laser pulses*

In this experiment, the filter used for beam1 was changed to a bandpass filter with a center wavelength of 700 nm with about 40 nm bandwidth. Beams 1 and 2 were characterized by the second-harmonic generation frequency-resolved optical-gating (SHG-FROG) method. The third beam (beam3) was used to measure pulse durations by the XFROG method with the two input beams and sidebands generation in a 10-μm-thick BBO crystal. Figure 7 depicts a retrieved XFROG trace showing the pulse durations of 40 ± 3 and 55 ± 3 fs for beam1 and beam2 being, respectively. The nearly equal pulse durations of the two input pulses guarantee that they are temporally well overlapped. The retrieved wavelength-dependent phase shows that beam2 has small positive chirp due to the dispersion of beam splitters and a lens. The spatial mode of the two input beams on the surface of the fused silica glass was measured with a CCD camera (Ophir Optronics BeamStar FX 33) and is shown in the inset of Fig. 8. Beams with elliptical cross sections were obtained by adjusting the beams at the edges of both of the lens and the concave mirror. Then, the two beams were aligned to overlap well by monitoring them using the CCD. The elliptical shapes of the beams make the two input beams to be overlapped well in the medium even though there was a crossing angle between them.

Multicolored cascaded FWM signals appeared separately in space outside of the two input beams when beam1 and beam2 were synchronously focused on the fused silica glass in both time and space. The photograph at the top of Fig. 9(a) shows the FWM sideband signals on a white sheet of paper placed about 30 cm after the glass plate. The input powers of beam1 and beam2 were 9 and 20 mW, respectively. An optical fiber was used to pick up different order signals to measure their spectra using a multichannel spectrometer (Ocean Optics USB4000). Figure 9(a) shows the spectra of the wavelengths of the sidebands from the first-Stokes (S1) to the fourth-order anti-Stokes (AS4) cascaded FWM signals together with the spectra of two input beams when the crossing angle between the two input beams was 1.87°. The spectrum extends from 450 to 1000 nm. The sidebands have a Gaussian profile and each anti-Stokes spectrum can support a transform-limited pulse duration of about 25 fs. Moreover, the wavelengths of the sidebands can be tuned easily by changing the crossing angle between the two input beams. In the experiment, beam2 was fixed and the crossing angle was changed by moving the position of beam1 on the surface of the concave mirror before the fused silica glass. It can be seen from Fig. 9(b) that the peak wavelength of AS3 can be tuned from 490 to 545 nm by changing the crossing angles from 1.40 to 2.57°. Comparing with the experiment described in §3.1, the wavelength tunable region was narrower due to the narrower spectral bandwidth of beam2. The crossing angles between the two neighboring sidebands decreased as the order number increased for a given crossing angle between the two beams. The crossing angle between beam2 and each beam of the sidebands was increased with the crossing angle of the two incident beams. The slope representing the dependence becomes steeper with increasing order number.

For the cascaded FWM, the m-order sideband should obey the energy conservation and momentum conservation laws: $(m+1)\omega_1 - m\omega_2 = \omega_{ASm}$ and $k_{ASm} - (k_1 - k_2) = k_{AS(m-1)}$, respectively. Here, 2 and 1 refer to the two input laser beams, ASm refers to the generated m-order anti-Stokes sideband. For an m-order Stokes sideband, the energy conservation and momentum conservation laws are $(m+1)\omega_2 - m\omega_1 = \omega_{Sm}$ and $k_{Sm} - (k_2 - k_1) = k_{S(m-1)}$, respectively.

The output pulse energies of AS1 and S1 were 1.03 and 1.05 μJ, respectively, when the crossing angle between the

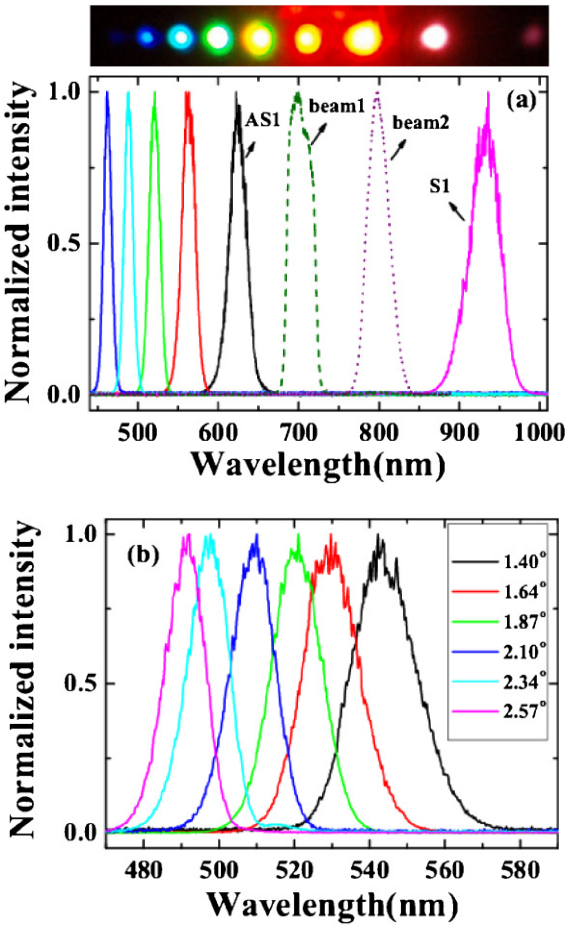

Fig. 9. (Color online) (a) Spectra of five sidebands from S1 through AS5 and of the two input beams when the crossing angle between the two input beams was 1.87°. (b) Spectra of AS3 at crossing angles of 1.40, 1.64, 1.87, 2.10, 2.34, and 2.57°. The photograph at the top of Fig. 9(a) shows the sidebands on a sheet of white paper placed 30 cm after the glass plate when the crossing angle was 1.87°. The first, second, and third spots from the right edge correspond to S1, beam2, and beam1, respectively.

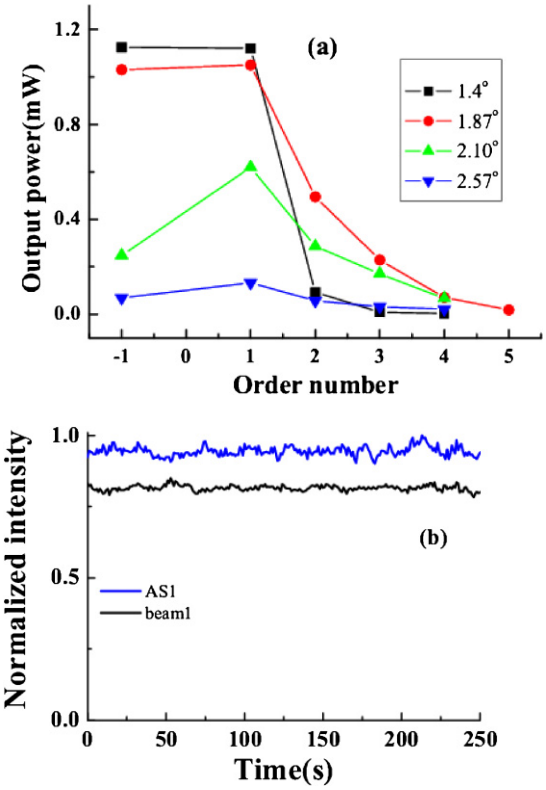

Fig. 10. (Color online) (a) Dependence of output power on order number when crossing angles between the two input beams were 1.40, 1.87, 2.10, and 2.57°. −1 refers to S1, 1 refers to AS1, and so on. (b) The power stabilities in terms of standard deviation of AS1 and beam1 monitored for over four minutes were determined to be 1.82 and 0.97% RMS, respectively.

input beams was 1.87° and the input powers of beam1 and beam2 were 9 and 20 mW, respectively. The output power of sideband is related to the crossing angle between the two input beams and the order number of sidebands. Figure 10(a) shows the dependence of the output power on order number when the crossing angles between the two input beams were 1.40, 1.87, 2.10, and 2.57°. The output powers of S1 and AS1 decreased rapidly with increasing crossing angle from 1.40 to 2.57°. For a smaller crossing angle between the two input beams, for example 1.40°, the output power of sidebands decreased rapidly with the increasing order number. In contrast, for a larger crossing angle between the two input beams, for example, 2.57°, the output power of sidebands decreased slowly with increasing order number. The energy conversion efficiency from the input beams to sideband beams in the process was about 10% when the crossing angle between the two input beams was 1.87°. The total conversion efficiency from the two pump pulses to all of the sidebands was about 10%. When the input power of beam2 was increased to 30 mW, An AS1 sideband as high as 1.15 mW was obtained. When a 0.5-mm-thick fused silica glass was used as a medium, the output power of AS1 decreased to about 0.5 mW. When the input power of beam2 was decreased to 15 mW, the output power of AS1 was about 0.95 mW. Even under such a low pump power excitation, the output power of beam2 did not decrease substantially. These phenomena indicate that the output power of sidebands is not sensitive to the input power of beam2, as concluded in a previous report. The standard deviations of fluctuations of AS1 and beam1 power monitored for over four minutes were 1.82 and 0.97% RMS, respectively, as shown in Fig. 10(b).

The pulse durations of S1, AS1, and AS2 were measured by generating cross-correlation signals with beam3 and then retrieving the XFROG trace using the commercial FROG software from Femtosoft Technologies. The recovered intensity profiles and phases of AS1 and AS2 were retrieved with errors of 0.012 and 0.010, respectively. The recovered pulse durations of AS1 and AS2 were 45 ± 3 and 44 ± 3 fs, respectively. The recovered pulse duration was 46 ± 3 fs with a retrieval error of 0.005. All the generated sidebands thus have similar pulse durations. The retrieved phase shows that there was chirp in the pulses due to the small positive chirp of input pulses and the dispersion of the glass.

Transform-limited sidebands may be obtained when the input pulses have small negative chirped with the same absolute value to compensate the dispersion of the glass.

The spatial modes of sidebands were also measured with the CCD camera. All the sidebands have a Gaussian spatial profile even though the two input beams have elliptic cross sections. This spatial mode improvement may be due to the combined effects of FWM, coherent anti-Stokes Raman scattering (CARS), cross-phase modulation (XPM), and self-phase modulation (SPM), in fused silica glass.

4. Conclusions

We experimentally generated spectrally and spatially well separated multicolored femtosecond laser pulses by a cascaded FWM process in a piece of fused silica glass. The wavelength can be continuously tuned by changing the crossing angle between two incident beams. The properties of the generated pulses were found to be good enough for different types of experiments. The output power of the sidebands can be increased easily by increasing the input power and the diameter on the glass. Moreover, it also can be amplified by another four-wave optical parametric amplification system.

Furthermore, multicolored femtosecond pulses of a μJ-level were obtained at the same time by the cascaded FWM process. A laser pulse of about 45 fs was obtained at around 950 nm. The energy conversion efficiency from the input beams to sidebands was about 10%. The properties of the generated sidebands made them suitable for various experiments, for example, a multicolor pump–probe experiment. This cascaded FWM process can be extended to different kinds of condensed isotropic media and to UV wavelengths, which is difficult to be obtained by using a nonlinear crystal because of the requirement of a rigorous phase-matching condition.

Acknowledgements

This work was partly supported by the 21st Century COE program on "Coherent Optical Science" and partly supported by a grant from the Ministry of Education (MOE) in Taiwan under the ATU Program at National Chiao Tung University. A part of this work was performed under the joint research project of Laser Engineering, Osaka University, under contract subject B1-27.

References

1) T. Kobayashi, A. Shirakawa, and T. Fuji: IEEE J. Sel. Top. Quantum Electron. **17** (2001) 525.
2) A. Baltuška, T. Fuji, and T. Kobayashi: Opt. Lett. **27** (2002) 306.
3) D. Brida, G. Cirmi, C. Manzoni, S. Bonora, P. Villoresi, S. De Silvestri, and G. Cerullo: Opt. Lett. **33** (2008) 741.
4) F. Thèberge, N. Aközbek, W. Liu, A. Becker, and S. L. Chin: Phys. Rev. Lett. **97** (2006) 023904.
5) T. Fuji, T. Horio, and T. Suzuki: Opt. Lett. **32** (2007) 2481.
6) T. Fuji and T. Suzuki: Opt. Lett. **32** (2007) 3330.
7) H. Crespo, J. T. Mendonça, and A. Dos Santos: Opt. Lett. **25** (2000) 829.
8) J. Liu and T. Kobayashi: Opt. Express **16** (2008) 22119.
9) M. Zhi and A. V. Sokolov: Opt. Lett. **32** (2007) 2251.
10) J. Liu, J. Zhang, and T. Kobayashi: Opt. Lett. **33** (2008) 1494.
11) M. Zhi, X. Wang, and A. V. Sokolov: Opt. Express **16** (2008) 12139.
12) E. Matsubara, T. Sekikawa, and M. Yamashita: Appl. Phys. Lett. **92** (2008) 071104.
13) H. Matsuki, K. Inoue, and E. Hanamura: Phys. Rev. B **75** (2007) 024102.
14) M. Zhi and A. V. Sokolov: New J. Phys. **10** (2008) 025032.
15) H. Valtna, G. Tamošauskas, A. Dubietis, and A. Piskarskas: Opt. Lett. **33** (2008) 971.
16) A. Dubietis, G. Tamošauskas, P. Polesana, G. Valiulis, H. Valtna, D. Faccio, P. Di Trapani, and A. Piskarskas: Opt. Express **15** (2007) 11126.
17) D. Pestov, R. K. Murawski, G. O. Ariunbold, X. Wang, M. C. Zhi, A. V. Sokolov, V. A. Sautenkov, Y. V. Rostovtsev, A. Dogariu, Y. Huang, and M. O. Scully: Science **316** (2007) 265.
18) R. M. Hochstrasser: Proc. Natl. Acad. Sci. U.S.A. **104** (2007) 14190.
19) R. Zgadzaj, E. Gaul, N. H. Matlis, G. Shvets, and M. C. Downer: J. Opt. Soc. Am. B **21** (2004) 1559.
20) C. Manzoni, D. Polli, and G. Cerullo: Rev. Sci. Instrum. **77** (2007) 023103.
21) H. Crespo and R. Weigand: Proc. 26th Int. Conf. Ultrafast Phenomena (UP, 2008), paper frilp-5.